Reactions of O_2^{2+} with CO_2, OCS and CS_2 ☆

Michael A. Parkes, Jessica F. Lockyear [1], Stephen D. Price [*]

University College London, Department of Chemistry, 20 Gordon Street, London WC1H 0AJ, UK

A B S T R A C T

The reactivity of O_2^{2+} with CO_2, OCS and CS_2 has been investigated for the first time, at centre-of-mass collision energies of 7.0, 7.9 and 8.5 eV, respectively. The position-sensitive coincidence technique we employ shows the reactivity in the three collision systems is dominated by double- and single-electron transfer. Analysis of the observed electron transfer reactivity indicates that the two-electron transfer is concerted and the translational energy does not couple efficiently to the electronic co-ordinates. In the O_2^{2+} + OCS collision system we observe a channel forming a new chemical bond, generating $SO^+ + CO^+ + O$. The angular scattering in this channel indicates that this reaction proceeds *via* complexation, then fragmentation of the complex to form $SO_2^+ + CO^+$. The primary SO_2^+ product then dissociates to $SO^+ + O$. *Ab initio* calculations support the presence of a collision complex in the pathway to $SO^+ + CO^+ + O$. The single-electron transfer reactions are direct and the energy releases we extract for the subsequent dissociation of the primary products (*e.g.* $O_2^+ + CO_2^+$) show that the internal vibrational energy of the O_2^{2+} reactant does not participate in the reaction.

1. Introduction

The molecular oxygen dication (O_2^{2+}) has been predicted to play a role in Earth's ionosphere [1,2]. The chemistry of O_2^{2+} can influence the properties of ionospheric and other environments in two significant ways. Firstly, bimolecular reactions of O_2^{2+} can act as a source of new molecules and ions. Secondly, and perhaps more subtly, the bimolecular reactions of O_2^{2+} commonly form pairs of monocationic products, with these monocations possessing significant translational energies due to their mutual Coulomb repulsion. In their subsequent encounters with atoms and molecules, the significant translational energies of these energized monocations may allow nominally endothermic reactions to occur. To characterize the role of O_2^{2+} in a variety of energized media we need to map out the form and energetics of its reactivity with prototypical molecules. The experimental work described in this paper provides a step towards this goal.

The double ionization of O_2 has been extensively studied using double charge transfer [3–5], Auger [6,7], photoelectron [8–13], photoion-photoion coincidence [14–16], photoelectron-photoion-photoion coincidence [17], electron ionization [7,18–22]

and Doppler-free kinetic-energy release [23] spectroscopies. In addition, femtosecond lasers have been used to study nuclear wave-packet dynamics in O_2^{2+} [24]. These investigations have led to a detailed understanding of the structure of the low-lying electronic states of O_2^{2+}. For example, the ground electronic state ($^1\Sigma_g^+$) of O_2^{2+} possesses a deep, metastable potential energy minimum (3.6 eV) [8,23,25,26]. The pre-dissociative lifetimes of dications with comparably deep metastable wells are measured to be at least of the order of seconds [27]. Such lifetimes are clearly sufficient to allow bimolecular collisions of O_2^{2+} with other molecules.

The fact that O_2^{2+} and O^+ have identical mass to charge ratios makes experimental investigations of the bimolecular reactivity of O_2^{2+} problematic, as "pure" beams of the dication are hard to prepare. Due to this experimental difficulty, the bimolecular reactivity of O_2^{2+} has received little attention [28–31]. The reaction of O_2^{2+} with N_2 has been studied in a selected ion flow tube (SIFT), where Glosik et al. [28] were able to determine that removal of the dication occurred at close to the collisional rate, assuming the dication reacted to form $O_2^+ + N_2^+$. Chatterjee and Johnsen [29] have studied the reactions of O_2^{2+} with O_2, N_2, CO_2, NO and Ne using a selected ion drift tube (SIDT) observing the formation of NO_2^+ following collisions of O_2^{2+} with NO. Coincidence studies, using the same methodology as employed in the current experiments, showed that, following single-electron transfer between O_2^{2+} and O_2, the O_2^+ formed from the neutral O_2 reactant was more likely to dissociate than the O_2^+ formed from the O_2^{2+} reactant [30].

In the experimental technique employed in this work a beam of O_2^{2+} encounters a jet of neutral molecules and the pairs of monocations formed in such encounters are detected in coincidence at a position-sensitive detector (PSD) [30–40]. This coincident

* Corresponding author.
E-mail address: s.d.price@ucl.ac.uk (S.D. Price).
[1] Current address: Lawrence Berkeley National Laboratories, 1 Cyclotron Road, Berkeley, CA 94720, USA.

detection of monocation pairs allows the distinction of the reactions of O_2^{2+} from any reactions of O^+. Thus, the reactivity of O_2^{2+} can be probed without requiring isotopic substitution to create a pure beam of dications [39]. This position-sensitive coincidence (PSCO) technique allows the determination of the nascent velocities of the product ion pairs on an event-by-event basis [39]. Such measurements have proven a detailed probe of the reactivity and reaction mechanisms of atomic and molecular dications [33,34]. Given the recent interest in the ionospheric role of molecular dications [2], and following an investigation of the chemistry of N_2^{2+}, which has provided data relevant for the ion chemistry of Titan [41,42], we have begun a study of the reactions of O_2^{2+} with various neutral molecules. This paper provides further results from this programme.

Following the interaction of a dication with a neutral, at low collision-energies, there are three main reaction pathways that can occur: double-electron transfer (DET), single-electron transfer (SET) and bond-forming reactions. Here we define "bond-forming" reactions to involve the exchange of atoms between the reactants accompanied by the formation of new chemical bonds.

$O_2^{2+} + CO_2 \rightarrow O_2^+ + CO_2^+$	Non-dissociative SET	Reaction 1
$O_2^{2+} + CO_2 \rightarrow O_2^+ + CO_2^{+*}, CO_2^{+*} \rightarrow CO^+ + O$	Dissociative SET	Reaction 2
$O_2^{2+} + CS_2 \rightarrow O_2 + CS_2^{2+}, CS_2^{2+} \rightarrow CS^+ + S^+$	Dissociative DET	Reaction 3
$O_2^{2+} + OCS \rightarrow SO^+ + CO^+ + O$	Bond forming reaction	Reaction 4

SET reactions (Reactions 1 and 2) between dications and neutrals have been extensively investigated [36,43,44]. The single-electron transfer is usually direct and occurs at long-range (3–6 Å) [45]. This SET reactivity is well represented by a simple model based on Landau–Zener theory [43,45]. The long-range nature of the electron transfer, in the vast majority of dicationic collision systems, results in strong forward scattering. We distinguish between non-dissociative SET, which results in simply a pair of primary product monocations ions (Reaction 1) and dissociative SET (Reaction 2) where at least one of the primary monocationic products subsequently fragments yielding a secondary monocation and at least one additional neutral species.

Considering DET, there have been recent hints that, at low collision energies, the transfer of the two electrons between the reactants generally occurs in a concerted manner; rather than by two sequential single-electron transfers [33]. We note that, since our PSCO technique detects pairs of product ions in coincidence, only dissociative DET reactions (Reaction 3) appear in our coincidence dataset. However, as discussed further below, any significant yields of long-lived product dications from DET (*e.g.* CS_2^{2+}) should be observable in the simple mass spectra we record in parallel with this coincidence data.

This paper reports the reactivity we observe following PSCO experiments to study collisions of O_2^{2+} with CO_2, OCS and CS_2 at low centre-of-mass (CM) collision energies. We observe bond-forming reactivity between O_2^{2+} and OCS, efficient two-electron transfer which appears to proceed by a concerted pathway between O_2^{2+} and both OCS and CS_2, and clear indications that the vibrational energy of the reactant O_2^{2+} dication does not dramatically influence the form of the single-electron transfer reactivity in any of the collision systems.

2. Experimental methodology and data analysis

Details of the PSCO experiment have been presented before [36,37,39]. In brief, dications are generated from a suitable precursor gas by electron ionization in a home-built ion source. Any cations produced in the source are electrostatically extracted and focused before energy-selection using a hemispherical energy-analyser. The energy-selected ions are then pulsed by sweeping the beam across a small aperture. These ion pulses are subsequently accelerated and focused into a commercial velocity filter [46]. The velocity filter is set to transmit only ions of a certain mass-to-charge ratio, in this case O_2^{2+} ($m/z = 16$) dications but also, unavoidably, O^+ monocations at the same m/z ratio The resulting beam of energy and mass-selected ions is decelerated and focused into the source region of a time-of-flight mass spectrometer (TOFMS). The TOFMS is orientated so that its major axis is aligned with the direction of the dication beam.

In the source region of the TOFMS the dications interact with an effusive jet of neutral molecules under single collision conditions. The interaction region is kept field-free as a dication pulse enters, so that any reactions occur at the intended low collision energy. Once the pulse of dications has reached the centre of the interaction region, a voltage is applied to a repeller plate to accelerate all the ions in the source region (product ions and unreacted reactant ions) into the TOFMS. The magnitude of this repeller plate voltage is chosen to ensure that all ions in the ion source reach the detector regardless of their initial velocity.

At the end of the TOFMS the ions are detected using a position-sensitive detector (PSD). The PSD measures an ion's time of arrival at a pair of micro-channel plates. Positional information is provided by a wire-wound delay line anode (RoentDek DLD80) positioned behind the plates. When two ion signals are detected following a repeller plate pulse, they are recorded as a coincidence and their positional information and flight times (t_1, t_2) are stored. If only a single ion is detected then its time-of-flight is simply added to a time-of-flight mass spectrum. The experimental event rate is kept low to ensure that true coincidences, where the pair of ions detected come from a single reactive event, are dominant over false coincidences. False coincidences occur when two ions formed in separate reactive events are detected as a pair. One consequence of the O^+ ions that unavoidably contaminate our dication beam, is that the coincidence data contains a significant number of false coincidences at precisely the flight time of these unreacted O^+ ions. These false coincidences can be readily identified and rejected without significant losses of true coincidences involving O^+ ions formed from reactions of O_2^{2+}. This distinction is possible because the O^+ ions from reactions of O_2^{2+} have a significant range of flight times and few real coincidence events are lost by rejecting ions with the narrow range of flight times of the O^+ ions present in the reactant beam.

The components of each product ion's velocity perpendicular to the axis of the TOFMS are derived from the position of the ionic impacts at the detector, whilst the on-axis component can be determined from the deviation of the measured ionic TOF from the TOF the ion would have if it was formed with zero initial kinetic energy [39]. These laboratory frame velocities are then converted to velocities in the CM frame $w(X^+)$ for ease of interpretation. This conversion is carried out using the velocity of the CM in the laboratory frame, which is determined from either the initial dication velocity or the velocities of the products of a reactive channel forming only two monocations (a two-body reaction, see below) [39].

Dication collisions that result in just a pair of monocations are termed two-body reactions. Conservation of momentum in the CM frame restricts the two monocations formed in a two-body reaction to having equal and opposite momenta in the CM frame (*e.g.* Reaction 1). In a three-body reaction a *single* neutral product is formed in addition to the pair of monocations (*e.g.* Reaction 2). A major advantage of the PSCO methodology is that, for these three body reactions, conservation of momentum in the CM frame allows the determination of the CM velocity of the neutral species from the velocities of the pair of product ions. Thus, for a three-body reaction, we can determine the velocities of all the products, and examine the correlations between these velocities to probe the reaction mechanism
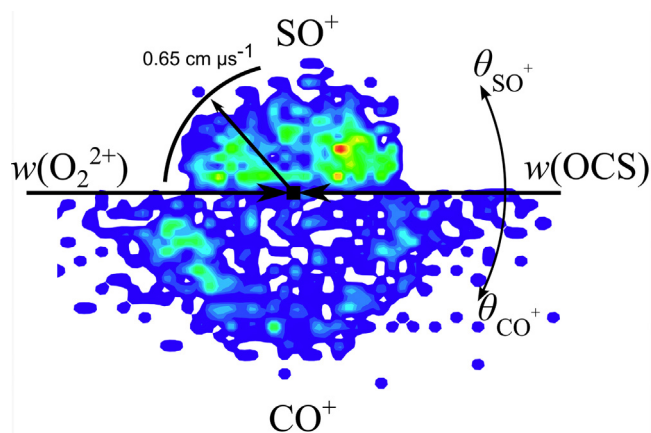
Fig. 1. CM scattering diagram of the SO^+ and CO^+ product ions following the reaction of O_2^{2+} and OCS. The diagram is a polar plot that shows the orientation of the velocities of the SO^+ and CO^+ products with respect to the direction of the reactant velocities, $w(O_2^{2+})$ and $w(OCS)$. $w(SO^+)$ and $w(CO^+)$ have maxima at 0.35 and 0.65 cm μs^{-1}, respectively. See text for details.

Fig. 2. Internal-frame scattering diagram of the SO^+ and O products relative to $w(CO^+)$. This diagram is a polar plot that shows the orientation of the SO^+ and O velocities relative to the CO^+ velocity, $w(CO^+)$. The location of the CM is indicated by the black square. The velocity of the nascent SO_2^{+*} ion, which subsequently fragments to SO^+ and O^+ is also indicated. See text for details.

and associated dynamics. This approach has proven very successful and has allowed exploration of a wide range of dicationic reaction mechanisms [36–39].

The first step in the analysis of the coincidence data from a given experiment is to plot a pairs spectrum, a two-dimensional mass spectrum, a histogram of t_1 vs. t_2 vs. counts. The different reactions occurring following the dication–neutral collisions appear as peaks in the pairs spectrum. A single pairs spectrum allows easy identification of all the reactive channels forming pairs of monocations from the given collision system at the experimental collision energy. We then select the experimental events corresponding to a specific reactive channel and inspect the correlations between the product velocities to investigate the channel's dynamics. For such an exploration we usually use two different types of scattering diagram. These scattering diagrams are simply polar histograms, assembled for all the reactive events collected for the channel of interest.

The first type of scattering diagram displays the angular scattering of the products in the CM frame. Here, for a product ion X^+, $|w(X^+)|$ is plotted as the radial coordinate and the scattering angle θ ($0 \leq \theta \leq 180°$) between the product's velocity vector and the velocity of the CM is plotted as the angular co-ordinate. Typically, the data for one product is displayed in the upper semi-circle of the diagram and the data for a second product is plotted in the lower semi-circle, an example is shown in Fig. 1 [39].

The second class of scattering diagram shows the scattering of one product (e.g. X^+) with respect to the velocity of another product (e.g. Y); an *internal frame* scattering diagram (Fig. 2). Here $|w(X^+)|$ is still used as the radial coordinate but the angular co-ordinate is now the angle ϕ ($0 \leq \phi \leq 180°$) between $w(X^+)$ and $w(Y)$. Internal frame scattering diagrams have proven particularly powerful for revealing the reaction mechanisms following dication–neutral interactions [33,36,37,47].

For three-body reactions, some valuable energetic information is accessible from the PSCO data. Following the reaction of AB^{2+} with C, two monocations, AB^{+*} and C^+ are formed, where AB^{+*} has enough energy to dissociate and $A^+ + C^+$ are detected as the final products. For such systems [30], we can determine the velocity of the dissociating ion, $w(AB^{+*})$, via conservation of momentum from the measured value of $w(C^+)$. Subtracting $w(AB^{+*})$ from the velocities of A^+ and B then yields the velocity vectors of A^+ and B in the frame of AB^+ allowing access to the kinetic energy (T_{int}) released in the fragmentation of AB^+, referred to as the internal kinetic energy release. The values of T_{int} can be directly compared to the known
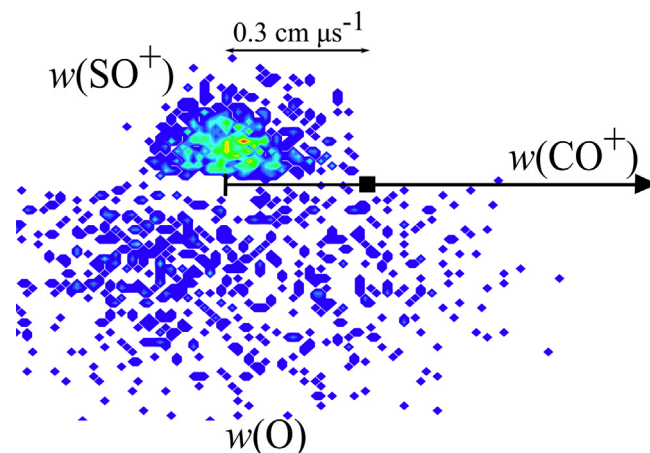
kinetic energy releases observed when an isolated AB^+ molecule dissociates, allowing identification of the states of AB^{+*} populated in the SET reaction.

When we consider the energetics of the reactions of O_2^{2+} it is important to note that the O_2^{2+} reactants will possess a range of internal energies. Previous studies have shown that, in comparable experiments, the reactant O_2^{2+} ions are in their ground electronic state ($^1\Sigma_g^+$) with the majority of ions distributed over vibrational levels with $v = 0$–6, with $v = 3$ having the highest population [8,26,48].

Apart from the carbon disulphide sample, the other reagents used in this study were >99% pure and were used without further purification. CS_2 was purified with a series of cool-pump-warm cycles to remove any dissolved air. We recorded PSCO spectra following collisions of an O_2^{2+} beam with the three target molecules at CM collision energies of 7.0 eV, 7.8 eV and 8.6 eV in the $O_2^{2+} + CO_2$, the $O_2^{2+} + OCS$ and the $O_2^{2+} + CS_2$ collision systems, respectively.

3. Results

Tables 1–3 list the product channels, with respective branching ratios, that we observe following collisions of O_2^{2+} with CO_2, OCS and CS_2. Table 1 shows that all four reaction channels observed in the O_2^{2+}/CO_2 collision system are due to SET; no DET or bond-forming reactions are detected. Table 2 shows that nine product channels are observed following collisions of O_2^{2+} with OCS. Channel 2.1, forming CO^+ and S^+, is due to DET from OCS to O_2^{2+}. Channel 2.9 is a bond-forming reaction generating SO^+, CO^+ and O. The remaining seven channels are a result of SET. The DET and chemical channels both have branching ratios of the order of 10%.

Five product channels (Table 3) are observed from the O_2^{2+}/CS_2 collision system. Two channels (Channels 3.1 and 3.2) are the result of DET, while all the other channels are due to SET reactions.

Table 1
Reaction channels following collisions O_2^{2+} with CO_2 at a centre-of-mass collision energy of 7.0 eV. The experimentally determined branching ratios and modal values of the internal kinetic energy releases (T_{int}) are also reported. See text for details.

	Products	Branching ratio	T_{int} (eV)
1.1	$CO_2^+ + O_2^+$	0.49	–
1.2	$CO_2^+ + O^+ + O$	0.10	0.4
1.3	$O_2^+ + O^+ + CO$	0.21	0.1
1.4	$O_2^+ + CO^+ + O$	0.20	0.1

Table 2
Reaction channels following collisions O_2^{2+} with OCS at a centre-of-mass collision energy of 7.8 eV. The experimentally determined branching ratios and modal values of the internal kinetic energy releases (T_{int}) are also reported. See text for details.

	Products	Branching ratio	T_{int} (eV)
2.1	$S^+ + CO^+ + O_2$	0.11	–
2.2	$OCS^+ + O_2^+$	0.01	–
2.3	$OCS^+ + O^+ + O$	0.30	1
2.4	$O_2^+ + CO^+ + S$	0.11	0.7
2.5	$O_2^+ + S^+ + CO$	0.30	0.5
2.6	$O_2^+ + O^+ + CS$	0.01	0.2
2.7	$O_2^+ + CS^+ + O$	0.03	0.1
2.8	$S^+ + O^+ + CO + O$	0.06	–
2.9	$SO^+ + CO^+ + O$	0.07	3.8

Table 3
Reaction channels following collisions O_2^{2+} with CS_2 at a centre-of-mass collision energy of 8.5 eV. The experimentally determined branching ratios and modal values of the internal kinetic energy releases (T_{int}) are also given. See text for details.

	Products	Branching ratio	T_{int} (eV)
3.1	$CS_2^{2+} + O_2$	0.41	–
3.2	$CS^+ + S^+ + O_2$	0.21	–
3.3	$CS_2^+ + O_2^+$	0.01	–
3.4	$CS_2^+ + O^+ + O$	0.26	2.8
3.5	$CS^+ + O_2^+ + S$	0.07	0.3
3.6	$O_2^+ + S^+ + CS$	0.04	0.4

Channel 3.1 forms long-lived CS_2^{2+} ions which only appear in our TOF mass spectrum, not, of course, in the pairs spectrum. If we have $I[CS_2^{2+}]$ dication counts in the mass spectrum due to non-dissociative DET and $P[CS^+ + S^+]$ pairs in the pairs spectrum due to dissociative DET, the ratio of dissociative to non-dissociative DET events is given by $P[CS^+ + S^+]/(f_i I[CS_2^{2+}])$ [49,50]; where f_i is the ion detection efficiency of the PSCO apparatus [49,50]. A recent study of the number of triples and pairs recorded by the PSCO apparatus following reactions of atomic trications allowed an estimation of the value of f_i for our apparatus as 0.15, a value consistent with other determinations for related detector assemblies [49,50]. Thus, we can place the intensity of the non-dissociative DET channel on the same scale as all the other processes that appear in the pairs spectrum, giving the branching ratios reported in Table 3. These branching ratios show that DET is clearly the most likely outcome of collisions of O_2^{2+} with CS_2.

4. Discussion

4.1. Bond-forming reactivity

Following the reaction of O_2^{2+} with OCS a single bond-forming reaction was observed (Channel 2.9) generating $SO^+ + CO^+ + O$. Fig. 1 shows the CM frame scattering of the SO^+ and CO^+ products for this reaction. The scattering is evenly distributed over the entire range of scattering angles (0–180°). This symmetrical scattering, over all scattering angles, clearly shows that the formation of $SO^+ + CO^+ + O$ proceeds *via* a collision complex which survives for several rotational periods [51]. The formation of such collision complexes is often implicated in the mechanisms for bond-forming reactivity in dication–neutral collisions [32,47,52].

The internal frame scattering diagram for this reaction (Fig. 2) clearly shows the SO^+ and O are scattered isotropically around a velocity vector of ~0.3 cm μs^{-1}. This precursor velocity is oriented in the opposite direction to $w(CO^+)$. We interpret this form of scattering as revealing that the $SO^+ + O$ products arise from the fragmentation of an energized precursor ion which the data indicates has a modal velocity of 0.3 cm μs^{-1}. Our data show that the modal value of $w(CO^+)$ for this reaction is 0.65 cm μs^{-1}. Thus, if the initial fragmentation of the collision complex was into $CO^+ + SO_2^{+*}$,
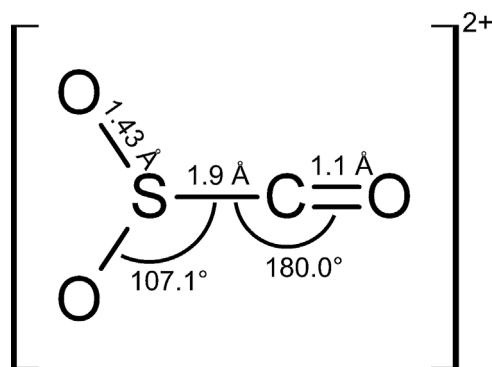

Fig. 3. The C_{2v} geometry of the $^1[O_2\text{-SCO}]^{2+}$ collision complex revealed by electronic structure calculations.

conservation of momentum indicates the SO_2^{+*} ion would have a modal velocity of 0.28 cm μs^{-1} if it completely separated from its CO^+ partner before fragmenting into $SO^+ + O$. This predicted value of $w(SO_2^{+*})$ agrees well with the value of $w(SO_2^{+*})$ revealed by the scattering diagram. Thus, our data clearly that indicate the bond forming reaction proceeds *via* the pathway:

$$O_2^{2+} + OCS \rightarrow [O_2\text{-OCS}]^{2+} \rightarrow CO^+ + SO_2^{+*} \rightarrow CO^+ + SO^+ + O$$
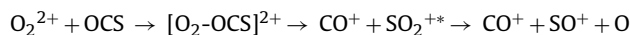
No other possible mechanism, sequential or concerted, for the formation of $SO^+ + CO^+ + O$ gives scattering in any way consistent with the experimental data. Given their significant internal energy, we expect the lifetimes of this collision complex, and the excited SO_2^{+*} ion, to be far too short for their detection as discrete ion masses in our TOFMS [53].

To support our experimental conclusions a computational study of the $O_2^{2+} + OCS$ reaction system was performed using Gaussian 09 [54]. Stationary points were located and characterized using a MP2(fc)/aug-cc-pVTZ methodology, and the energies of these stationary points were then determined using a CCSD(T) algorithm employing the same basis set. For reactions of O_2^{2+}, in its ground singlet state, with OCS an accessible collision complex was located (Fig. 3). The complex has a C_{2v} structure and an energy of 9.91 eV below the reactant asymptote. In this complex (Fig. 3) the O—O bond has ruptured and the oxygen atoms have added across the sulphur atom, this addition is associated with a dramatic lengthening of the S—C bond. This lengthening strongly hints that this complex is poised to dissociate to $SO_2^+ + CO^+$, in accord with the experimental data. To confirm this deduction we also located a transition state which connects the complex shown in Fig. 3 to separated SO_2^+ and CO^+. However, further investigation revealed that the electronic structure of the transition state may be better represented by a multi-reference wavefunction, so we do not report its details here. Nevertheless, the results of this preliminary computational investigation support the experimentally determined reaction pathway to $SO^+ + CO^+ + O$.

4.2. Double-electron transfer reactions

As shown in Tables 1–3, DET reactions are observed following collisions of O_2^{2+} with OCS and CS_2 but not with CO_2. This absence of a DET reaction in the $O_2^{2+} + CO_2$ system can be explained by simple energetics. The formation of $CO_2^{2+} + O_2$ from $O_2^{2+}(^1\Sigma_g^+) + CO_2$ is endothermic by 1.2 eV [8,55]. In contrast, both OCS and CS_2 have double ionization energies below that of O_2^{2+}, making DET in these collision systems an exothermic process by 6.1 eV and 9.2 eV, respectively [11,56]. The absence of any DET reactivity between O_2^{2+} and CO_2 clearly shows that the collision energy (in this case 7.0 eV) and the vibrational energy of O_2^{2+} do not couple with electronic degrees of freedom to allow the nominally endothermic

formation of CO_2^{2+} to occur with observable intensity. Indeed, the fact that the collision energy does not efficiently couple to the electronic degrees of freedom in dicationic single-electron transfer reactivity has been noted before [33].

Our data (Table 2) reveal the DET reaction between O_2^{2+} and OCS gives S^+ and CO^+ (channel 2.1) exclusively; no other ion pairs due to DET are observed in the pairs spectrum and no hint of OCS^{2+} appears above the noise level in the mass spectrum. Energetically, and assuming that the collision energy does not couple with the electronic energy, DET from ground-state O_2^{2+} can populate OCS^{2+} states with energies (relative to ground state OCS) of up to 36.1 eV. From the velocity vectors of the CO^+ and S^+, an average kinetic energy release of 5.1 eV is determined for the fragmentation of the OCS^{2+} dication, formed by DET, to S^+ and CO^+. By adding this energy release to the energy of the CO^+ and S^+ asymptote (27.6 eV) we estimate the energy of the OCS^{2+} electronic state populated in the DET process is 32.7 eV, close to the top of the barrier in the $CO^+ + S^+$ dissociation pathway of the $\tilde{a}^1\Delta$ state [56]. Further support for this DET process populating high lying vibrational levels of $OCS^{2+}(\tilde{a}^1\Delta)$, is given by the fact that the kinetic energy release we derive for the formation of $S^+ + CO^+$ agrees well with earlier experimental and theoretical values for fragmentation of OCS^{2+} from this state (5.1 eV and 5.44 eV, respectively) [56].

We have previously considered the mechanism of DET between a dication and a neutral in a study of the reactions of Ar^{2+} with C_2H_2 [33]. The DET reactivity of the $Ar^{2+} + C_2H_2$ collision system could be best understood if the two-electron transfer was a concerted two-electron process; a direct crossing from the reactant $Ar^{2+} + C_2H_2$ potential energy surface to the product $Ar + C_2H_2^{2+}$ surface, rather than a sequential process *via* an intermediate $[Ar^+ + C_2H_2^+]$ state. Modelling the reactant and product potentials for $O_2^{2+} + OCS \rightarrow O_2 + OCS^{2+}$ with a simple polarization-attraction we see that the exothermicity (3.4 eV) for populating the excited vibrational states of $OCS^{2+}(\tilde{a}^1\Delta)$ from O_2^{2+} places the crossing between these potentials at approximately 2.4 Å, well within the so-called reaction window for efficient electron transfer used to rationalize DET in our previous work [33,36,43]. Other known decay pathways of OCS^{2+} (*e.g.* to $S^+ + C^+ + O$) occur from OCS^{2+} states which are energetically inaccessible to our collision system, again assuming the separation of translational and electronic degrees of freedom, and are thus not observed in our experiments [56]. We note that a larger exothermicity (3.4 eV) is determined for the DET reaction we observe in the O_2^{2+}/OCS collision system than the almost thermoneutral DET processes that occur in the Ar^{2+}/C_2H_2 system [33]. This difference arises due to the markedly larger polarizability of OCS than O_2, whereas for Ar^{2+}/C_2H_2 the polarizabilites of Ar and C_2H_2 are very similar. When there is a significant difference in the polarizability of the neutral reactant (OCS) and product (O_2) molecules, a significant energetic separation between the reactant and product asymptotes is required to position a DET curve crossing within the reaction window.

The above analysis would predict that the CS_2^{2+} states populated by DET in the O_2^{2+}/CS_2 collision system will involve even larger exothermicities than in the reactions with OCS, as the polarizability of CS_2 (8.8 Å³) is even larger than that of OCS (5.5 Å³). Our results are in excellent agreement with this prediction (Table 3). We observe efficient DET to form $S^+ + CS^+$, a fragmentation of CS_2^{2+} for which we measure a kinetic energy release of 4.5 eV. This energy release is in good agreement with the value of 4.3 eV measured by Lablanquie et al. following dissociative photoionization of CS_2 at 33.5 eV [57]; an energy release associated with the population of high-lying vibrational levels of the ground $\tilde{X}^3\Sigma_g^-$ state of CS_2^{2+} which rapidly dissociate to $CS^+ + S^+$ [58]. The exothermicity for forming CS_2^{2+} in these states from the reaction of O_2^{2+} and CS_2 is 5.3 eV placing the curve crossing for DET again close to 2.4 Å. This value of the crossing

radius is almost identical to the value of the crossing radius for efficient DET in the O_2^{2+} and OCS system. As noted above, in our earlier investigation of DET reactivity in the Ar^{2+}/C_2H_2 collision system efficient two-electron transfer was observed [33]. For the Ar^{2+}/C_2H_2 collision system we estimate the relevant two-electron curve crossings lie at an interspecies separation of approximately 2.7 Å Thus, all the efficient DET processes we have investigated to date possess very similar radii for the associated two-electron transfer curve crossings (2.4–2.7 Å); an observation lending support to the concerted mechanism for the DET process.

Our results also show (Table 3) that DET processes have a markedly larger branching ratio for the reactions of O_2^{2+} with CS_2 than in the O_2^{2+}/OCS collision system. That DET is more favourable for the CS_2 reaction is consistent with the large double ionization cross-section for this molecule [59].

4.3. Single-electron transfer

SET reactions make a significant contribution to the product ion flux following reactions of O_2^{2+} with all three target molecules (CO_2, OCS and CS_2). The PSCO data for all these SET reactions reveals strong forward scattering, consistent with direct electron transfer at a significant interspecies separations. As mentioned above, this form of scattering is commonly observed for dication–neutral SET reactions [33,36,37,40,43].

There has been recent interest in how energy is partitioned between the products of dicationic SET reactions [30,31]. It is especially interesting to investigate how the internal energy of the reactants influences the SET reactivity. The distributions of T_{int}, the kinetic energy release for the dissociation of the nascent monocationic products formed in the primary SET step between O_2^{2+} and CO_2, are shown in Fig. 4. Fig. 4(a) shows a large range of energy releases for the dissociation of the O_2^+ product, peaking at low energies but extending above 4 eV. However, a much more restricted range of energy releases are apparent for the fragmentation of the primary CO_2^+ product of the electron transfer process (Fig. 4(b) and (c)). The distribution of energy releases for the fragmentation of the O_2^+ is strikingly similar to that previously determined for the fragmentation of the O_2^+ ion (the capture monocation) formed from the O_2^{2+} reactant following collisions of O_2^{2+} with O_2 [30]. The T_{int} distributions we observe following the SET reactions of O_2^{2+} with OCS and CS_2 are similar to those illustrated in Fig. 4 with the primary O_2^+ product fragmenting with a very broad range of kinetic energies whilst most of the OCS^+ and CS_2^+ fragmentations have energy releases of less than 1 eV (see Supplementary Information). The similarity of the O_2^+ kinetic energy release (KER) distributions upon fragmentation in the collision systems reported here and the KER distribution of the capture O_2^+ ion following SET between O_2^{2+} and O_2 strongly hints that the O_2^+ states populated when the reactant O_2^{2+} ion accepts an electron are broadly independent of the collision partner. This observation, and the fact that the KER distribution of the capture O_2^+ cannot be well represented by that of a vibrationless ion [30], points to the fact that the vibrational energy of the reactant O_2^{2+} ion is not efficiently transferred to the partner monocation (*e.g.* CO_2^+). Such a conclusion is perhaps not surprising as the SET process occurs when the reactants are at a significant interspecies separation, an interaction distance that is not conducive to vibrational energy flow between the reactants.

If the vibrational energy in the reactant O_2^{2+} is not passed to the reactant partner in the SET process, we would expect the T_{int}, distributions for the fragmentation of the partner CO_2^+, OCS^+ and CS_2^+ ions formed in the SET process to be very similar to those observed in photoionization of the corresponding neutral species. This is indeed the case. Liu et al. performed a high-resolution pulsed-field
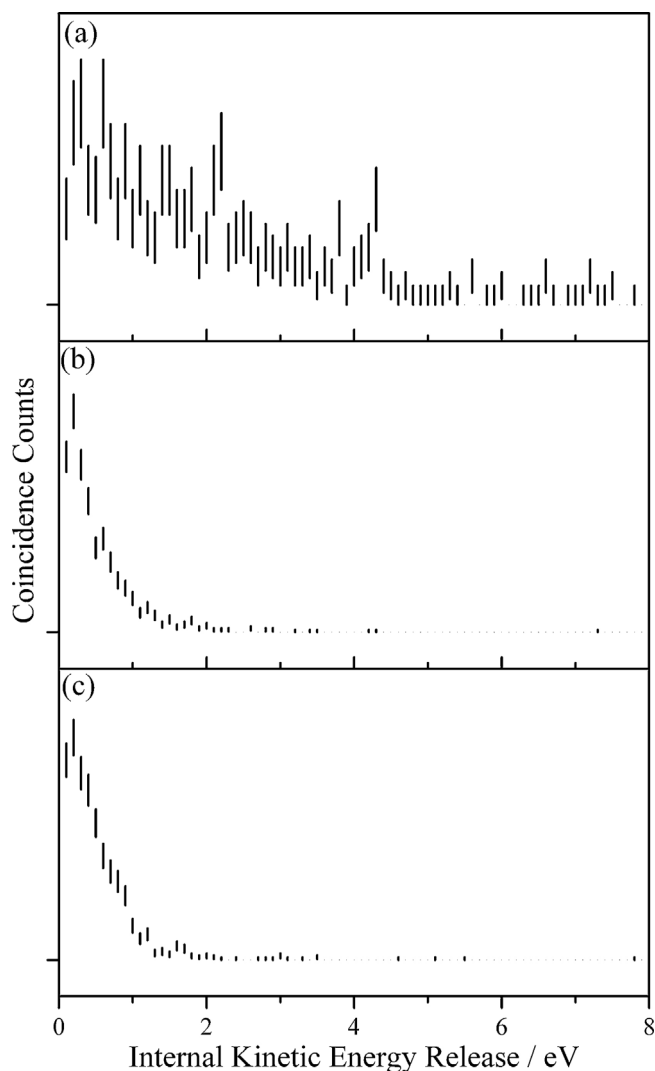
Fig. 4. Internal frame kinetic energy release (T_{int}) distributions for the dissociative SET reactions we observe following collisions of O_2^{2+} with CO_2 at a collision energy of 7.0 eV: (a) $O_2^+ \rightarrow O^+ + O$ following the formation of $CO_2^+ + O_2^{+*}$; (b) $CO_2^+ \rightarrow CO^+ + O$ and (c) $CO_2^+ \rightarrow O^+ + CO$ following the initial formation of $CO_2^{+*} + O_2^+$.

ionization measurement of the dissociation of CO_2^+ formed in low vibrational levels of the $\tilde{C}$ state [60]. They measured the average kinetic energy releases into $O^+ + CO$ and $CO^+ + O$ for each vibrational level. For $O^+ + CO$ their average release for all the vibrational levels was 0.3 eV while for dissociation to $CO^+ + O$ the average release was 0.1 eV. These values compare well with the modal values of our measured T_{int} distributions.

For the reaction of O_2^{2+} with OCS we observe (Table 2) four different SET channels forming an OCS^{+*} ion which dissociates, although the $CS^+ + O$ and $O^+ + CS$ channels are quite weak. The KERs of the $S^+ + CO$ and $CO^+ + S$ channels following the formation of OCS^+ by photoionization have been previously determined experimentally [61–63]. The formation of $S^+ + CO$ was studied over a range of different ionization energies (13.5–16.5 eV) where the KER was found to have values between 0.1 and 1 eV [62,63]. The formation of $CO^+ + S$ was examined only from the $\tilde{C}$ state of OCS^+ and the KER shows a bimodal distribution with peaks at 0.6 and 0.8 eV [61]. Our modal T_{int} values for these two channels (0.5 and 0.7 eV, respectively) agree well with the photoionization kinetic energy releases.

For the SET reactions in the O_2^{2+}/CS_2 collision system, our modal T_{int} value for dissociation to CS^+ and S (0.3 eV) agrees well with the

value of around 0.5 eV found by Brehm et al. [64] although the maximum energy release of ~2.0 eV is slightly higher than the maximum value of 1.2 eV observed by Aitchison and Eland [65]. The agreement between our T_{int} values and the photoionization data for the fragmentation of CS_2^{+*} to S^+ and CS is also good. Specifically, we measure a peak value of 0.4 eV for the T_{int} distribution which is close to the average value of 0.3 eV found by Brehm et al. [64]. Our maximum value of T_{int} for the fragmentation to $S^+ + CS$ is 1.5 eV which is in good agreement with the maximum value observed by Aitchison and Eland of 1.4 eV for dissociation from the $\tilde{C}$ state of CS_2^+.

Given the above analysis it seems clear from our data that, in these SET reactions, the electron capture by the dication and the electron loss from the neutral proceed as effectively independent processes. The loss of the electron from the neutral molecule appears well represented by ionization of an isolated species, whilst the vibrational energy content of the reactant dication does not appear to couple significantly with the neutral species. Of course, the electron capture by the dication and the ionization of the neutral are not in fact occurring in isolation. However, to a first approximation, it appears that the influence of one upon the other can be neglected in simple modelling of the energy content of the products of SET. This conclusion is in accord with previous work on the SET reactions of CO^{2+} [66]. More sensitive probes of the internal energy distributions of the products of SET are required to reveal any effect of the internal energy content of the reactants on the internal energy distributions of the products.

5. Conclusion

The reactions of CO_2 and its sulphur containing analogues (OCS and CS_2) with O_2^{2+} have been investigated. The major reactive channels in all three cases are found to be single (CO_2, OCS) or double (CS_2) electron transfer. The single-electron transfer takes place rapidly by a direct mechanism. As the number of sulphur atoms in the neutral reactant is increased the contribution of double-electron transfer to the product ion yield increases dramatically. The absence of double-electron transfer in the O_2^{2+} and CO_2 system clearly indicates that the collision energy of the reaction cannot promote this nominally endothermic process.

Following the reaction of O_2^{2+} with OCS we detect a bond-forming reaction generating $SO^+ + CO^+ + O$. The angular scattering we observe in this channel indicates that this reaction proceeds *via* complexation followed by initial fragmentation to $SO_2^+ + CO^+$. The SO_2^+ ion subsequently fragmenting to $SO^+ + O$. *Ab initio* calculations support the presence of a collision complex in the pathway to $SO^+ + CO^+ + O$.

Appendix A. Supplementary data

Supplementary data associated with this article can be found, in the online version, at http://dx.doi.org/10.1016/j.ijms.2013.06.018.

References

[1] C. Nicolas, C. Alcaraz, R. Thissen, J. Zabka, O. Dutuit, Planetary and Space Science 50 (2002) 877.
[2] C. Simon, J. Lilensten, O. Dutuit, R. Thissen, O. Witasse, C. Alcaraz, H. Soldi-Lose, Annals of Geophysics 23 (2005) 781.

[3] J. Appell, J. Durup, F.C. Fehsenfeld, P. Fournier, Journal of Physics B 6 (1973) 197.
[4] J. Fournier, P.G. Fournier, M.L. Langford, M. Mousselmal, J.M. Robbe, G. Gandara, Journal of Chemical Physics 96 (1992) 3594.
[5] O. Furuhashi, T. Kinugawa, T. Hirayama, T. Koizumi, C. Yamada, S. Ohtani, Physical Review A 70 (2004) 052501.
[6] W.E. Moddeman, T.A. Carlson, M.O. Krause, B.P. Pullen, W.E. Bull, G.K. Schweitzer, Journal of Chemical Physics 55 (1971) 2317.
[7] M. Larsson, P. Baltzer, S. Svensson, B. Wannberg, N. Martensson, A. Naves de Brito, N. Correia, M.P. Keane, M. Carlsson-Gothe, L. Karlsson, Journal of Physics B 23 (1990) 1175.
[8] R.I. Hall, G. Dawber, A. McConkey, M.A. Macdonald, G.C. King, Physical Review Letters 68 (1992) 2751.
[9] P. Bolognesi, D. Thompson, L. Avaldi, M. MacDonald, M. Lopes, D. Cooper, G. King, Physical Review Letters 82 (1999) 2075.
[10] S.D. Price, J.H.D. Eland, Journal of Physics B 24 (1991) 4379.
[11] J.H.D. Eland, Chemical Physics 294 (2003) 171.
[12] R. Feifel, J.H.D. Eland, Physical Review A 71 (2005) 034501.
[13] R. Feifel, J.H.D. Eland, D. Edvardsson, Journal of Chemical Physics 122 (2005) 144308.
[14] D.M. Curtis, J.H.D. Eland, International Journal of Mass Spectrometry and Ion Processes 63 (1985) 241.
[15] J.H.D. Eland, S.D. Price, J.C. Cheney, P. Lablanquie, I. Nenner, P.G. Fournier, Philosophical Transactions of the Royal Society of London, Series A 324 (1988) 247.
[16] A. Yamada, H. Fukuzawa, K. Motomura, X.-J. Liu, L. Foucar, M. Kurka, M. Okunishi, K. Ueda, N. Saito, H. Iwayama, K. Nagaya, A. Sugishima, H. Murakami, M. Yao, A. Rudenko, K.U. Kühnel, J. Ullrich, R. Feifel, A. Czasch, R. Dörner, M. Nagasono, A. Higashiya, M. Yabashi, T. Ishikawa, H. Ohashi, H. Kimura, T. Togashi, Journal of Chemical Physics 132 (2010) 204305.
[17] S. Hsieh, J.H.D. Eland, Journal of Physics B 29 (1996) 5795.
[18] F. Dorman, J. Morrison, Journal of Chemical Physics 39 (1963) 1906.
[19] J.H. Beynon, R.M.R. Caprioli, W. J, Journal of the American Chemical Society 93 (1971) 1852.
[20] T.D. Mark, Journal of Chemical Physics 63 (1975) 3731.
[21] B. Brehm, G. Frenes, International Journal of Mass Spectrometry and Ion Processes 26 (1978) 251.
[22] J.M. Curtis, R.K. Boyd, Journal of Chemical Physics 81 (1984) 2991.
[23] M. Lundqvist, D. Edvardsson, P. Baltzer, M. Larsson, B. Wannberg, Journal of Physics B 29 (1996) 499.
[24] S. De, I.A. Bocharova, M. Magrakvelidze, D. Ray, W. Cao, B. Bergues, U. Thumm, M.F. Kling, I. Litvinyuk, C. Cocke, Physical Review A 82 (2010) 013408.
[25] D. Edvardsson, S. Lunell, F. Rakowitz, C.M. Marian, L. Karlsson, Chemical Physics 229 (1998) 203.
[26] L.G.M. Pettersson, M. Larsson, Journal of Chemical Physics 94 (1991) 818.
[27] D. Mathur, L.H. Andersen, P. Hvelplund, D. Kella, C.P. Safvan, Journal of Physics B 28 (1995) 3415.
[28] J. Glosik, A.B. Rakshit, N.D. Twiddy, N.G. Adams, D. Smith, Journal of Physics B 11 (1978) 3365.
[29] B.K. Chatterjee, R. Johnsen, Journal of Chemical Physics 91 (1989) 1378.
[30] M.A. Parkes, J.F. Lockyear, S.D. Price, D. Schröder, J. Roithová, Z. Herman, Physical Chemistry Chemical Physics 12 (2010) 6233.
[31] M.A. Parkes, J.F. Lockyear, D. Schroder, J. Roithova, S.D. Price, Physical Chemistry Chemical Physics 13 (2011) 18386.
[32] J.F. Lockyear, C.L. Ricketts, M.A. Parkes, S.D. Price, Chemical Science 2 (2011) 150.
[33] M.A. Parkes, J.F. Lockyear, S.D. Price, International Journal of Mass Spectrometry 280 (2009) 85.
[34] J.F. Lockyear, M.A. Parkes, S.D. Price, Journal of Physics B 42 (2009) 145201.
[35] C.L. Ricketts, D. Schröder, J. Roithová, H. Schwarz, R. Thissen, O.D.J. Žabka, Z. Herman, S.D. Price, Physical Chemistry Chemical Physics 10 (2008) 5135.
[36] S.D. Price, International Journal of Mass Spectrometry 260 (2007) 1.
[37] W.P. Hu, S.M. Harper, S.D. Price, Molecular Physics 103 (2005) 1809.
[38] S.M. Harper, S.W.-P. Hu, S.D. Price, Journal of Chemical Physics 120 (2004) 7245.
[39] W.-P. Hu, S.M. Harper, S.D. Price, Measurement Science and Technology 13 (2002) 1512.
[40] S.M. Harper, W.-P. Hu, S.D. Price, Journal of Physics B 35 (2002) 4409.
[41] J. Lilensten, O. Witasse, C. Simon, H. Soldi-Lose, O. Dutuit, R. Thissen, C. Alcaraz, Geophysical Research Letters 32 (2005) 5.
[42] O. Dutuit, N. Carrasco, R. Thissen, V. Vuitton, C. Alcaraz, P. Pernot, N. Balucani, P. Casavecchia, A. Canosa, S. Le Picard, J.-C. Loison, Z. Herman, J. Zabka, D. Ascenzi, P. Tosi, P. Franceschi, S.D. Price, P. Lavvas, Astrophysical Journal Supplement Series 204 (2013) 20.
[43] Z. Herman, International Reviews in Physical Chemistry 15 (1996) 299.
[44] S.D. Price, Journal of the Chemical Society, Faraday Transactions 93 (1997) 2451.
[45] S.A. Rogers, S.D. Price, S.R. Leone, Journal of Chemical Physics 98 (1993) 280.
[46] L. Wåhlin, Nuclear Instruments and Methods in Physics Research 27 (1964) 55.
[47] J.F. Lockyear, M.A. Parkes, S.D. Price, Angewandte Chemie International Edition 50 (2011) 1322.
[48] P.J. Linstrom, W.G. Mallard, NIST Chemistry WebBook, NIST Standard Reference Database Number 69, National Institute of Standards and Technology, Gaithersburg, MD, 2008.
[49] P. Calandra, C.S.S. O'Connor, S.D. Price, Journal of Chemical Physics 112 (2000) 10821.
[50] S. Harper, P. Calandra, S.D. Price, Physical Chemistry Chemical Physics 3 (2001) 741.
[51] R.D. Levine, R.B. Bernstein:, Molecular Reaction Dynamics and Chemical Reactivity, Oxford University Press, Oxford, 1987.
[52] N. Tafadar, D. Kearney, S.D. Price, Journal of Chemical Physics 115 (2001) 8819.
[53] C.L. Ricketts, S.M. Harper, S.W.-P. Hu, S.D. Price, Journal of Chemical Physics 123 (2005) 134322.
[54] M.J. Frisch, G.W. Trucks, H.B. Schlegel, G.E. Scuseria, M.A. Robb, J.R. Cheeseman, G. Scalmani, V. Barone, B. Mennucci, G.A. Petersson, H. Nakatsuji, M. Caricato, X. Li, H.P. Hratchian, A.F. Izmaylov, J. Bloino, G. Zheng, J.L. Sonnenberg, M. Hada, M. Ehara, K. Toyota, R. Fukuda, J. Hasegawa, M. Ishida, T. Nakajima, Y. Honda, O. Kitao, H. Nakai, T. Vreven, J.A. Montgomery Jr., J.E. Peralta, F. Ogliaro, M. Bearpark, J.J. Heyd, E. Brothers, K.N. Kudin, V.N. Staroverov, R. Kobayashi, J. Normand, K. Raghavachari, A. Rendell, J.C. Burant, S.S. Iyengar, J. Tomasi, M. Cossi, N. Rega, J.M. Millam, M. Klene, J.E. Knox, J.B. Cross, V. Bakken, C. Adamo, J. Jaramillo, R. Gomperts, R.E. Stratmann, O. Yazyev, A.J. Austin, R. Cammi, C. Pomelli, J.W. Ochterski, R.L. Martin, K. Morokuma, V.G. Zakrzewski, G.A. Voth, P. Salvador, J.J. Dannenberg, S. Dapprich, A.D. Daniels, Ö. Farkas, J.B. Foresman, J.V. Ortiz, J. Cioslowski, D.J. Fox, Gaussian 09, Revision A. 1, Gaussian, Inc., Wallingford, CT, 2009.
[55] A.E. Slattery, T.A. Field, M. Ahmad, R.I. Hall, J. Lambourne, F. Penent, P. Lablanquie, J.H.D. Eland, Journal of Chemical Physics 122 (2005) 084317.
[56] V. Brites, J.H.D. Eland, M. Hochlaf, Chemical Physics 346 (2008) 23.
[57] P. Lablanquie, I. Nenner, P. Millie, P. Morin, J.H.D. Eland, M.J. Hubin-Franskin, J. Delwiche, Journal of Chemical Physics 82 (1985) 2951.
[58] S. Taylor, J.H.D. Eland, M. Hochlaf, Chemical Physics 330 (2006) 16.
[59] T.A. Field, J.H.D. Eland, Chemical Physics Letters 303 (1999) 144.
[60] J. Liu, W. Chen, M. Hochlaf, X. Qian, C. Chang, C.Y. Ng, Journal of Chemical Physics 118 (2003) 149.
[61] S. Morse, M. Takahashi, J.H.D. Eland, L. Karlsson, International Journal of Mass Spectrometry 184 (1999) 67.
[62] M.-J. Hubin-Franskin, J. Delwiche, P.-M. Guyon, M. Richard-Viard, M. Lavollée, O. Dutuit, J.-M. Robbe, J.-P. Flament, Chemical Physics 209 (1996) 143.
[63] B. Brehm, R. Frey, A. Küstler, J.H.D. Eland, International Journal of Mass Spectrometry and Ion Processes 13 (1974) 251.
[64] B. Brehm, J.H.D. Eland, R. Frey, A. Küstler, International Journal of Mass Spectrometry and Ion Processes 12 (1973) 213.
[65] D. Aitchison, J.H.D. Eland, Chemical Physics 263 (2001) 449.
[66] A. Ehbrecht, N. Mustafa, C. Ottinger, Z. Herman, Journal of Chemical Physics 105 (1996) 9833.